analytical chemistry

pubs.acs.org/ac Letter

Monitoring Chemical Reactions with SERS-Active Ag-Loaded Mesoporous TiO_2 Films

M. Mercedes Zalduendo, Víctor Oestreicher, Judith Langer, Luis M. Liz-Marzán, and Paula C. Angelomé*

Cite This: https://dx.doi.org/10.1021/acs.analchem.0c03310 Read Online

ACCESS | Metrics & More | Article Recommendations | Supporting Information

ABSTRACT: Monitoring chemical reactions that occur in small spaces or confined environments is challenging. Surface-enhanced Raman scattering (SERS) spectroscopy offers the unique possibility to monitor spectral changes with high sensitivity and time resolution. Herein, we report the application of composite mesoporous TiO_2 films loaded with Ag nanoparticles (NPs) to track *in situ* chemical processes in real time. In particular, the AgNPs@TiO_2 system was employed to monitor two chemical reactions: one occurring on the Ag NPs surface and another taking place in the surrounding solution. In the first case, we monitored the decarboxylation reaction of 4-mercaptobenzoic acid on Ag NPs, which allowed us to identify the conditions that favor it. In the second case, we studied the pH evolution in the nanocavities during a homogeneous alkalization process driven by chloride-assisted glycidol rupture (the Epoxide Route) and compared it with pH measurements by conventional techniques. We therefore demonstrated that the proposed nanodevice provides an excellent performance to monitor dynamic processes occurring either inside the material or in the solution in which it is immersed.

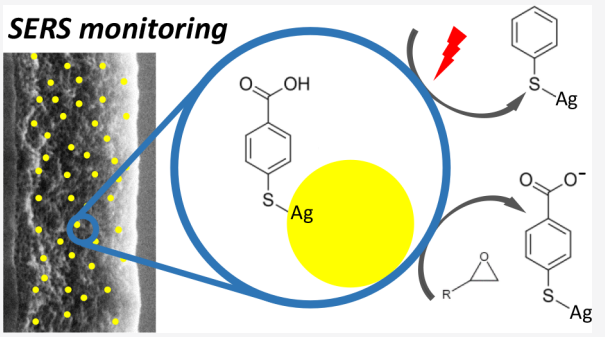

Monitoring chemical reactions that occur on nanoparticle surfaces or inside confined spaces is a subject of high current relevance. The obtained information has impact both on the physicochemical understanding of such processes and on their potential technological applications. Surface-enhanced Raman scattering (SERS) spectroscopy has proved to be a powerful analytical technique for such studies, mainly due to its surface selectivity, high sensitivity, and access to spectral information. Detailed studies in different complex environments can be achieved thanks to the size scale of the metallic nanoparticles (NPs) required for SERS, which is compatible with these domains. Diverse dynamic processes have been monitored *in situ* by SERS, including catalytic reactions,[1] electrochemical reactions,[2] and different biological processes,[3] among many others.[4] Various SERS sensors have been used to monitor chemical reactions, and typically, each application requires a specific platform design. For example, the use of SERS to follow catalytic reactions requires the nanostructure to be the active catalyst, while enhancing the Raman signal of reagents, products, or both.[1,5] Most such SERS platforms involve NPs of different sizes, anisotropic and bimetallic NPs, either in suspension or supported on solid surfaces. Another major example is the use of SERS to determine local pH and to monitor pH changes.[6−9] In this case, the challenge relies on designing a platform that is sufficiently sensitive to a specific pH range. For this purpose, molecules with different acid−base properties (dimercaptobenzoic acid, aminothiophenol, and mercaptopyridine, just to mention a few) have been assembled onto the surface of selected NPs and either pH-dependent molecular fingerprints or spectral changes were assigned to the corresponding pH values.[10] pH-SERS sensors involve mainly dispersed NPs, but the use of immobilized NPs has been reported.[6,11] In the latter case, the NP stability is improved, a key point since acid−base properties of pH reporters could be affected if the NP surface is modified.[12]

However, it would be useful to rely on a single and versatile platform to follow different chemical reactions with good performance, so that their potential applications can be expanded. In this respect, composite materials comprising mesoporous thin films and metal nanoparticles present a great potential, due to the wide variety of compositions and architectures that can be achieved.[13] One of the main advantages of building such composite materials is the support that the mesoporous film offers to metal NPs. Therefore, destabilization due to uncontrolled aggregation in solution is avoided while NPs remain in contact with the outer medium through the porosity of the film. The mesoporous film can further act as a molecular sieve protecting the SERS sensor

Received: August 4, 2020
Accepted: September 21, 2020
Published: September 21, 2020

https://dx.doi.org/10.1021/acs.analchem.0c03310
Anal. Chem. XXXX, XXX, XXX−XXX

against potentially interfering species, such as large proteins in biofluids.[14] Additionally, the high uniformity of mesoporous materials provides an excellent platform towards the study of chemical reactions occurring in confined spaces. On the other hand, these materials are robust and easy to handle, thereby allowing their incorporation into different reaction media.[15]

Mesoporous nanocomposites have been used as SERS sensors for the detection of various analytes;[15,16] most examples comprising *ex situ* experiments where it is not possible to sense changes in the reaction medium. We propose herein the use of nanocomposite films for real-time SERS-based monitoring of two different chemical reactions produced in confined environments, with equally good performance. As a proof of concept, the SERS probe molecule 4-mercaptobenzoic acid (MBA) was used to follow two different types of chemical reactions: (1) a catalytic process directly onto the NP surface and (2) a reaction that takes place in the surrounding medium, far away from the NP surface. In case 1, MBA covalently bound to Ag NPs undergoes a well-known decomposition reaction, whereas the NPs fulfill a double function, as a Raman signal amplifier and a catalyst for the reaction.[17] Intensity and spectral changes of the initial MBA SERS fingerprint directly reflect the ongoing transformation into the product. Then, in case 2, the formation of the reaction products induces a pH change in the solution where the sensor is immersed (Scheme S1, SI). Since pH affects the protonation state of MBA, characteristic features are observed in its vibrational fingerprint, so that it can be used to follow the evolution of the reaction.[6]

The composite material used as the SERS-active substrate is obtained by reducing $AgNO_3$ by formaldehyde inside a mesoporous TiO_2 thin film (thickness = 220 ± 10 nm), templated with the triblock copolymer Pluronic F127 (porosity = 45% ± 5%, pore diameter = 8 ± 1 nm; see SI for more details).[18] Amorphous TiO_2 was chosen as the support material since it presents good chemical and mechanical stability. Figure 1a shows the appearance of the obtained AgNPs@TiO_2 film, along with its UV−visible spectrum, featuring a broad plasmon band with an absorbance maximum at 463 nm, due to the presence of Ag NPs. TEM images (Figure 1b and Figure S1a, SI) indicate that NPs are embedded in the TiO_2 matrix and present an isotropic shape. Size analysis reveals a broad NP size distribution (Figure S1b, SI) with an average diameter of 7 ± 3 nm. X-ray reflectometry analysis indicates a Ag loading fraction of 18%, as well as accessibility for the diffusion of external molecules, as demonstrated for the case of water vapor (Figure S1c, SI).

The pH-sensitive SERS response of MBA has been extensively studied[19] and is demonstrated in Figure S2, SI, together with the corresponding band assignment (Table S1, SI). Three vibrational bands are used to determine the pH value: (i) the aromatic ring stretching at 1587−1591 cm^{-1} (aromatic 2), (ii) C═O stretching at 1650−1710 cm^{-1} (carboxylic group, COOH), and (iii) COO^- symmetric stretching (carboxylate group, COO^-) between 1370 and 1380 cm^{-1}. Further details of this analysis are provided in the Supporting Information.

A word of caution should be given regarding the use of MBA as a pH-SERS probe, since it can undergo catalytic decomposition through a decarboxylation process (a typical example of NP-mediated reactions). More specifically, the excitation with laser light can generate hot electrons at the NP surface, which can interact with bound MBA and trigger its transformation into thiophenol (TP) by the loss of CO_2 (Scheme S1, SI).[20] This process is readily observable—though not often acknowledged—by the appearance of vibrational bands at 1000, 1025, and 1575 cm^{-1}, which correspond to TP aromatic ring vibrations.[19] To study this reaction, the AgNPs@TiO_2 system was incubated with a MBA solution for 18 h and extensively washed to remove unbound molecules prior to SERS measurements with the platform immersed in phosphate buffer saline (PBS) solution (see SI for further details). Figure 2a shows SERS spectra of MBA, recorded at three different times on the same spot during constant irradiation over the entire measurement period.

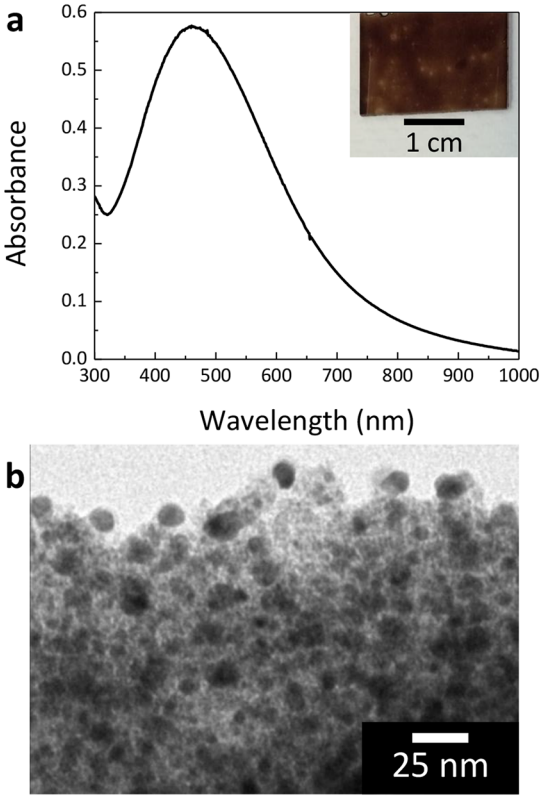

Figure 1. (a) UV−visible spectrum of AgNPs@TiO_2. Inset: Optical image of the sensor. (b) Representative TEM image of AgNPs@TiO_2.

Initially, the SERS spectrum of MBA could be detected, together with some additional vibrational peaks at 1000 and 1025 cm^{-1}, which can be attributed to the presence of TP. As irradiation time was increased, the intensity of TP bands increased so they could be readily distinguished from those of MBA. Simultaneously, a decrease in the intensity of the MBA carboxylate band could be observed. Shown in Figure 2b are signal intensities of MBA's COO^- band and the TP band at 1000 cm^{-1}, normalized to the 1080 cm^{-1} band, as a function of irradiation time. A continuous decrease of the carboxylate band intensity, accompanied by a steady increase of the TP band, was observed over a period of 100 s, indicating the reaction progress. Experiments carried out under different pH conditions, using different lasers and irradiation (excitation) powers, suggest that decarboxylation is favored if: the pH is near but above the pK_a of MBA, the laser intensity is increased, and the 633 nm laser is used. The effect of pH is related to the reaction mechanism, as previously reported.[17] Regarding the laser, the formation of TP was more evident when a 633 nm laser, with lower nominal power (Table S2, SI), was used

https://dx.doi.org/10.1021/acs.analchem.0c03310
Anal. Chem. XXXX, XXX, XXX−XXX

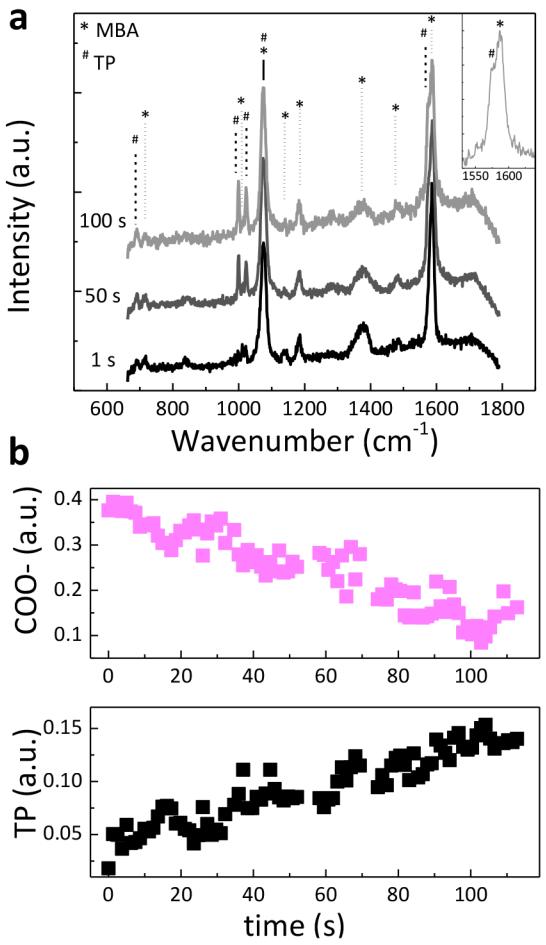

Figure 2. (a) SERS spectra of MBA and its decarboxylation product, TP, recorded at different times on a same spot, constantly irradiated over 100 s with a laser power of 6 mW. (b) Intensity of vibrational bands corresponding to TP (1000 cm^{-1}) and the carboxylate group of MBA, both normalized to the vibrational band at 1080 cm^{-1}, as a function of irradiation time. Measurement conditions: PBS 0.05 M, pH 6.2. Renishaw Raman microscope: 633 nm laser (50% filter), 50× long distance microscope, and 1 s acquisition time.

instead of a 532 nm laser. Since AgNPs@TiO_2 presents a broad plasmon extinction band, the presence of NPs of different sizes in close proximity is to be expected. Thus, our results indicate that the nanostructures excited with each laser are different and that those with a higher absorption coefficient at 633 nm have greater catalytic activity. It is important to highlight that TiO_2 films were treated at 200 °C and, thus, are amorphous; as a consequence, they do not present photocatalytic activity.[21] Therefore, the catalytic activity of the material originates from the Ag NPs. More details about the decarboxylation reaction under different measurement conditions and the relation of the results with the proposed mechanism are presented in the Supporting Information.

These results indicate that AgNPs@TiO_2 composites can both catalyze MBA decarboxylation and facilitate SERS-based monitoring of the reaction. Hence, we confirm that composite materials can be used to follow a reaction occurring directly on the NPs surface. From the obtained results, it is also clear that decarboxylation affects directly one of the variables typically used in the literature to measure pH: the intensity of the carboxylate band (COO^-). In fact, the intensity of this band decreases by ca. 75% during MBA degradation. Thus, experiments carried out under different conditions (laser wavelength, laser power, pH) allowed us to recognize which factors favor the decarboxylation reaction. At the same time, these results help us define the optimum acquisition conditions to perform pH measurements, since decarboxylation must be completely avoided if MBA is to be used as a pH reporter.

The next step comprises the use of a reaction that takes place in the bulk solution but has an effect over MBA immobilized on the NPs. We determined the pK_a value of MBA immobilized in the AgNPs@TiO_2 system, which was found to be 3.5−4.5, depending on the buffer concentration (Figure S3, SI). Therefore, this platform can be used to determine pH changes near the pK_a range. Taking into account the range of action, we selected for this purpose a homogeneous reaction that can gradually increase the pH of the medium: the Epoxide Route (Scheme S1, SI).[22] This reaction has been extensively employed in the past for the synthesis of layered hydroxides and hybrid materials.[23] In those cases, the alkalization kinetics can be tuned by choosing the initial pH, the initial concentrations of both reagents (epoxide and nucleophile), and the temperature.[24] Importantly, the reaction can also be followed by traditional, simple, and efficient pH measurement techniques so that we can have a suitable control over the reaction path, besides that offered by the SERS platform, which is sadly unusual in the literature.

Before using the AgNPs@TiO_2 system to follow the chloride-assisted glycidol rupture, the sensor was treated for 18 h with a 1 mM HCl solution to passivate the NPs surface.[25,26] This treatment guaranteed that no spectral change occurred during the chemical reaction (Figure S5, SI). The system was then incubated with MBA. The alkalization reaction was initiated by adding glycidol (the epoxide) to a solution containing sodium chloride (the nucleophile) at pH 3. The AgNPs@TiO_2 system was then immersed in an aliquot of the reaction mixture, and SERS spectra were recorded over time (see SI for detailed information), while another aliquot of this solution was kept as a control to monitor pH changes using a pH meter. As previously demonstrated, MBA can undergo a decarboxylation reaction. Measurement conditions were thus selected to avoid this process; a 514 nm laser was used for these experiments. Selected MBA SERS spectra obtained throughout the reaction are presented in Figure 3a. Initially, both the COOH band and the COO^- band could be observed, whereas at the end of the reaction (approximately after 37 min), only the COO^- vibration was detected. This means that, at the beginning of the reaction, at pH 3, neutral and deprotonated MBA molecules are in chemical equilibrium at the Ag NP surface, in accordance with the estimated pK_a value for MBA in the AgNPs@TiO_2 system in the reaction conditions (Figure S3, SI), wereas at the end, at pH 10, all molecules are in the deprotonated state, as expected. A more detailed analysis of the pH-sensitive vibrational bands (Figure 3b) shows that, at longer reaction times, the COO^- band increases in intensity while the aromatic 2 band is shifted toward lower wavenumbers. The changes in these two signals occur at similar time scales and are indicative of an increased pH in the medium, compatible with changes produced by the chemical reaction under study. Therefore, we can conclude that AgNPs@TiO_2 films provide enough sensitivity for *in situ* detection of pH changes produced by a chemical reaction occurring in the outer medium.

https://dx.doi.org/10.1021/acs.analchem.0c03310
Anal. Chem. XXXX, XXX, XXX−XXX

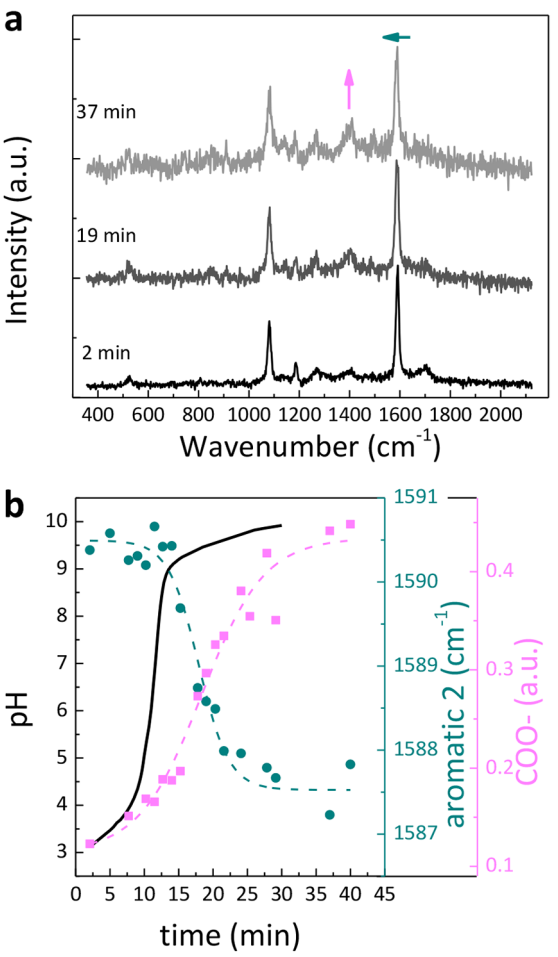

Figure 3. (a) SERS spectra of MBA during glycidol rupture reaction (NaCl 150 mM and glycidol 750 mM, starting pH 3). Arrows indicate spectral changes observed during the reaction. (b) Vibrational spectra analysis: intensity of carboxylate group and aromatic 2 bands as a function of time (dashed lines are a guide for the eye). The pH curve obtained with a pH meter is also shown (black solid line). Measurement conditions: Horiba equipment, 514 nm laser (100% intensity), 50× long distance objective, and 30 s (2 accumulations) or 20 s (3 accumulations) acquisition times.

An important remark about these results is that the observed changes in SERS spectra due to pH differences during glycidol rupture start after an abrupt change in pH observed by pH meter measurements. Given that the pK_a of MBA in these systems is below 5, SERS spectra are expected to change before rather than after this abrupt change. This delay may be due to MBA deprotonation kinetics, to diffusion processes, and/or to confinement effects related to the mesoporous material. Preliminary results suggest that the kinetics of immobilized MBA acid−base equilibrium play a major role. However, further studies are required to fully understand the origin of this behavior.

In conclusion, we demonstrated that composite systems comprising metal nanoparticles and mesoporous thin films can be used to track *in situ* different chemical reactions in real time. In particular, we provided data using the AgNPs@TiO_2 system to monitor two reactions. First, a decarboxylation reaction catalyzed by the plasmonic NPs surface, which also amplifies the Raman signal. Second, we monitored pH changes associated with a process taking place in the outer medium in which the sensor is immersed: an alkalization process driven by the Epoxide Route. Therefore, the proposed composite systems were used to monitor dynamic processes occurring both inside and outside the mesoporous structure and on the surface of the NPs or in the solution in which they are immersed. Interestingly, the structural and chemical parameters of the composites can be tailored by changing the precursors used for the synthesis, thereby offering promising use in the study of a wide variety of confined chemical reactions. Finally, SERS provides spectral information on the involved molecular species, thereby allowing the determination of reaction mechanisms or other processes occurring at the confined nanoscale. Moreover, the potential of this composite system relies on its feasibility to be immersed in different complex media without compromising NPs stability.

■ ASSOCIATED CONTENT

Supporting Information

The Supporting Information is available free of charge at https://pubs.acs.org/doi/10.1021/acs.analchem.0c03310.

Experimental section, AgNPs@TiO_2 system characterization and stability, MBA spectra and pK_a, and MBA decarboxylation under different conditions with mechanism details (PDF)

■ AUTHOR INFORMATION

Corresponding Author

Paula C. Angelomé − *Gerencia Química & Instituto de Nanociencia y Nanotecnología, Centro Atómico Constituyentes, Comisión Nacional de Energía Atómica, CONICET, Buenos Aires, Argentina;* orcid.org/0000-0002-4402-5045; Email: angelome@cnea.gov.ar

Authors

M. Mercedes Zalduendo − *Gerencia Química & Instituto de Nanociencia y Nanotecnología, Centro Atómico Constituyentes, Comisión Nacional de Energía Atómica, CONICET, Buenos Aires, Argentina*

Víctor Oestreicher − *Gerencia Química & Instituto de Nanociencia y Nanotecnología, Centro Atómico Constituyentes, Comisión Nacional de Energía Atómica, CONICET, Buenos Aires, Argentina; Instituto de Ciencia Molecular (ICMol), Universidad de Valencia, 46980 Valencia, Spain;* orcid.org/0000-0003-1636-4565

Judith Langer − *CIC biomaGUNE and CIBER-BBN, Basque Research and Technology Alliance (BRTA), 20014 Donostia-San Sebastián, Spain*

Luis M. Liz-Marzán − *CIC biomaGUNE and CIBER-BBN, Basque Research and Technology Alliance (BRTA), 20014 Donostia-San Sebastián, Spain; Ikerbasque, Basque Foundation for Science, 48013 Bilbao, Spain;* orcid.org/0000-0002-6647-1353

Complete contact information is available at: https://pubs.acs.org/10.1021/acs.analchem.0c03310

Notes

The authors declare no competing financial interest.

■ ACKNOWLEDGMENTS

This work was supported by ANPCyT (PICT 2015-0351). M.M.Z. acknowledges CONICET for her doctoral fellowship. M.M.Z. and P.C.A thank Dr. E. B. Halac (Departamento de

Física de la Materia Condensada, CAC, CNEA) for access to the Raman equipment. L.M.L.-M. acknowledges funding by the Spanish State Research Agency, under Grant No. MAT2017-86659-R and the María de Maeztu Units of Excellence Program (MDM-2017-0720).

REFERENCES

(1) Zhang, Z.; Deckert-Gaudig, T.; Deckert, V. *Analyst* **2015**, *140* (13), 4325−4335.
(2) Wu, D.-Y.; Li, J.-F.; Ren, B.; Tian, Z.-Q. *Chem. Soc. Rev.* **2008**, *37* (5), 1025−1041.
(3) Cui, L.; Zhang, D.; Yang, K.; Zhang, X.; Zhu, Y.-G. *Anal. Chem.* **2019**, *91* (24), 15345−15354.
(4) Langer, J.; Jimenez de Aberasturi, D.; Aizpurua, J.; Alvarez-Puebla, R. A.; Auguie, B.; Baumberg, J. J.; Bazan, G. C.; Bell, S. E. J.; Boisen, A.; Brolo, A. G.; Choo, J.; Cialla-May, D.; Deckert, V.; Fabris, L.; Faulds, K.; Garcia de Abajo, F. J.; Goodacre, R.; Graham, D.; Haes, A. J.; Haynes, C. L.; Huck, C.; Itoh, T.; Kall, M.; Kneipp, J.; Kotov, N. A.; Kuang, H.; Le Ru, E. C.; Lee, H. K.; Li, J.-F.; Ling, X. Y.; Maier, S. A.; Mayerhofer, T.; Moskovits, M.; Murakoshi, K.; Nam, J.-M.; Nie, S.; Ozaki, Y.; Pastoriza-Santos, I.; Perez-Juste, J.; Popp, J.; Pucci, A.; Reich, S.; Ren, B.; Schatz, G. C.; Shegai, T.; Schlucker, S.; Tay, L.-L.; Thomas, K. G.; Tian, Z.-Q.; Van Duyne, R. P.; Vo-Dinh, T.; Wang, Y.; Willets, K. A.; Xu, C.; Xu, H.; Xu, Y.; Yamamoto, Y. S.; Zhao, B.; Liz-Marzan, L. M. *ACS Nano* **2020**, *14* (1), 28−117.
(5) Xie, W.; Schlücker, S. *Chem. Commun.* **2018**, *54* (19), 2326−2336.
(6) Kneipp, J.; Kneipp, H.; Wittig, B.; Kneipp, K. *J. Phys. Chem. C* **2010**, *114* (16), 7421−7426.
(7) Zhang, Z.; Bando, K.; Mochizuki, K.; Taguchi, A.; Fujita, K.; Kawata, S. *Anal. Chem.* **2019**, *91* (5), 3254−3262.
(8) Luo, R.; Li, Y.; Zhou, Q.; Zheng, J.; Ma, D.; Tang, P.; Yang, S.; Qing, Z.; Yang, R. *Analyst* **2016**, *141* (11), 3224−3227.
(9) Bálint, Š.; Rao, S.; Marro, M.; Miškovský, P.; Petrov, D. *J. Raman Spectrosc.* **2011**, *42* (6), 1215−1221.
(10) Huang, Y.; Liu, W.; Wang, D.; Gong, Z.; Fan, M. *Microchem. J.* **2020**, *154*, 104565.
(11) Xu, M.; Ma, X.; Wei, T.; Lu, Z.-X.; Ren, B. *Anal. Chem.* **2018**, *90* (23), 13922−13928.
(12) Litti, L.; Reguera, J.; García de Abajo, F. J.; Meneghetti, M.; Liz-Marzan, L. M. *Nanoscale Horizons* **2020**, *5*, 102−108.
(13) Zalduendo, M. M.; Langer, J.; Giner-Casares, J. J.; Halac, E. B.; Soler-Illia, G. J. A. A.; Liz-Marzán, L. M.; Angelomé, P. C. *J. Phys. Chem. C* **2018**, *122* (24), 13095−13105.
(14) López-Puente, V.; Abalde-Cela, S.; Angelomé, P. C.; Alvarez-Puebla, R. A.; Liz-Marzán, L. M. *J. Phys. Chem. Lett.* **2013**, *4* (16), 2715−2720.
(15) Angelomé, P. C.; Fuertes, M. C. Metal Nanoparticles-Mesoporous Oxide Nanocomposite Thin Films. In *Handbook of Sol-Gel Science and Technology*; Klein, L., Aparicio, M., Jitianu, A., Eds.; Springer International Publishing: Cham, 2018; pp 2507−2533.
(16) Innocenzi, P.; Malfatti, L. *TrAC, Trends Anal. Chem.* **2019**, *114*, 233−241.
(17) Zong, Y.; Guo, Q.; Xu, M.; Yuan, Y.; Gu, R.; Yao, J. *RSC Adv.* **2014**, *4* (60), 31810−31816.
(18) Fuertes, M. C.; Marchena, M.; Marchi, M. C.; Wolosiuk, A.; Soler-Illia, G. J. A. A. *Small* **2009**, *5* (2), 272−280.
(19) Michota, A.; Bukowska, J. *J. Raman Spectrosc.* **2003**, *34* (1), 21−25.
(20) Huh, H.; Trinh, H. D.; Lee, D.; Yoon, S. *ACS Appl. Mater. Interfaces* **2019**, *11* (27), 24715−24724.
(21) Angelomé, P. C.; Andrini, L.; Calvo, M. E.; Requejo, F. G.; Bilmes, S. A.; Soler-Illia, G. J. A. A. *J. Phys. Chem. C* **2007**, *111* (29), 10886−10893.
(22) Oestreicher, V.; Jobbágy, M. *Langmuir* **2013**, *29* (39), 12104−12109.
(23) Oestreicher, V.; Jobbagy, M. *Chem. - Eur. J.* **2019**, *25*, 12611−12619.
(24) Oestreicher, V.; Jobbágy, M. *Chem. Commun.* **2017**, *53* (24), 3466−3468.
(25) Li, L.; Zhu, Y.-J. *J. Colloid Interface Sci.* **2006**, *303* (2), 415−418.
(26) Siskova, K.; Becicka, O.; Safarova, K.; Zboril, R. HCl Effect on Two Types of Ag Nanoparticles Utilizable in Detection of Low Concentrations of Organic Species. In *Sustainable Nanotechnology and the Environment: Advances and Achievements*; Shamim, N., Sharma, V. K., Eds.; ACS Symposium Series 1124; American Chemical Society: Washington, DC; 2013; pp 151−163.

https://dx.doi.org/10.1021/acs.analchem.0c03310
Anal. Chem. XXXX, XXX, XXX−XXX